American Journal of Pathology, Vol. 151, No. 4, October 1997

Increased Oxidative DNA Damage and Hepatocyte Overexpression of Specific Cytochrome P450 Isoforms in Hepatitis of Mice Infected with *Helicobacter hepaticus*

Marek A. Sipowicz,* Pascale Chomarat,† Bhalchandra A. Diwan,‡ Miriam A. Anver,‡ Yogesh C. Awasthi,§ Jerrold M. Ward,¶ Jerry M. Rice,* Kazimierz S. Kasprzak,* Christopher P. Wild,† and Lucy M. Anderson*

From the Laboratory of Comparative Carcinogenesis, Frederick Cancer Research and Development Center, Veterinary and Tumor Pathology Section, Animal Sciences Branch, ¶Division of Basic Sciences, National Cancer Institute, Frederick, Maryland; the Unit on Environmental Carcinogenesis, International Agency for Research on Cancer,† Lyon, France; the SAIC-Frederick, NCI-FCRDC,‡ Frederick, Maryland; and the University of Texas Medical Branch,§ Galveston, Texas*

A recently discovered bacterium, *Helicobacter hepaticus*, infects the intrahepatic bile canaliculi of mice, causing a severe chronic hepatitis culminating in liver cancer. Thus, it affords an animal model for study of bacteria-associated tumorigenesis including *H. pylori*-related gastric cancer. Reactive oxygen species are often postulated to contribute to this process. We now report that hepatitis of male mice infected with *H. hepaticus* show significant increases in the oxidatively damaged DNA deoxynucleoside 8-hydroxydeoxyguanosine, with the degree of damage increasing with progression of the disease. Perfusion of infected livers with nitro blue tetrazolium revealed that superoxide was produced in the cytoplasm of hepatocytes, especially in association with plasmacytic infiltrates near portal triads. Contrary to expectations, Kupffer cells, macrophages, and neutrophils were rarely involved. However, levels of cytochrome P450 (CYP) isoforms 1A2 and 2A5 in hepatocytes appeared to be greatly increased, as indicated by the number of cells positive in immunohistochemistry and the intensity of staining in many cells, concomitant with severe hepatitis. The CYP2A5 immunohistochemical staining co-localized with formazan deposits resulting from nitro blue tetrazolium reduction and occurred in nuclei as well as cytoplasm. These findings suggest that CYP2A5 contributes to the superoxide production and 8-hydroxydeoxyguanosine formation, although reactive oxygen species from an unknown source in the hepatocytes leading to CYP2A5 induction or coincidental occurrence of these events are also possibilities. Three glutathione *S*-transferase isoforms, mGSTP1–1 (pi), mGSTA1–1 (YaYa), and mGSTA4–4, also showed striking increases evidencing major oxidative stress in these livers. *(Am J Pathol 1997, 151:933–941)*

Increased risk of cancer has been associated with infection of the liver by human hepatitis viruses[1] and liver flukes,[2] the bladder by schistosome parasites,[2] and the gastric epithelium by the bacterium *Helicobacter pylori*.[2,3] Recently a new murine *Helicobacter* species, *H. hepaticus*, was discovered as the causative agent of severe progressive hepatitis and liver tumorigenesis,[4,5] providing for the first time an animal model for bacteria-related carcinogenesis.

H. hepaticus-associated hepatitis is much more common in male than female mice and shows mouse strain specificity in that C57BL/6 mice are resistant.[4,6–8] The natural history of this disease has been studied in greatest detail in strain A/J mice in which it was first discovered. The bacteria are apparently transmitted by the fecal-oral route early in life. Disease progression is slow, characterized by focal, low-grade necrosis and nonsuppurative inflammation at ages 1 to 6 months.[6–8] Lesions become more severe by 8 months with more extensive necrosis and a distinctive pericholangitis, including bile ductule hyperplasia, and prominent peribiliary inflammatory cells. Monocytes are particularly abundant,[6,7] but macrophages and neutrophils may also accumulate.[8] By

Supported in part by National Institute of Environmental Health Sciences Grant ES06052 to C. P. Wild. P. Chomarat was supported by a Special Training Award from the IARC and by the Ligur National Contre de Cancer.

Accepted for publication June 24, 1997.

Address reprint requests to Dr. Lucy M. Anderson, National Cancer Institute, Frederick Cancer Research and Development Center, Building 538, Room 205E, Frederick, MD 21702. Tel.: 301-846-5600; Fax: 301-846-5946; E-mail: andersol@ncifcrf.gov

Current address for J. M. Rice is the Unit of Carcinogen Identification and Evaluation, International Agency for Research on Cancer, Lyon, France.

Current address for C. P. Wild is the Molecular Epidemiology Unit, Research School of Medicine, University of Leeds, Leeds, United Kingdom.

Current address for M. A. Sipowicz is the Institute of Obstetrics and Gynecology, Medical School, Sklodowskiej 24A, 15-246 Bialystok, Poland.

12 months of age, altered preneoplastic foci and adenomas are seen; neoplasms are found in 75 to 100% of male mice by 18 months.[4,8] Serum antibodies appear approximately at the time when the disease becomes active and marked lymphocytic infiltrates are noted (6 to 8 months of age), reaching a maximum coincident with the first appearance of tumors in males (12 months).[6,8]

Thus, the mice mount an immune response with inflammation against *H. hepaticus*, albeit one that does not forestall severe liver disease indefinitely in most mouse strains. Inflammatory reactions often entail increased production of reactive oxygen species (ROS). The latter have been postulated to be tumorigenic due in part to their ability to cause promutagenic DNA damage.[9] ROS are also an usual part of tissue response to tumor promoter treatment; these may contribute to promotion by clastogenic and/or epigenetic actions.[10] Therefore, we investigated whether ROS increased during *H. hepaticus* infection and liver tumorigenesis as indicated by levels of the promutagenic oxidized nucleoside 8-hydroxydeoxyguanosine (8-oxo-dG) in hepatic DNA and *in situ* generation of superoxide by liver perfusion with nitro blue tetrazolium (NBT).[11,12] In addition, because several cytochrome P450 (CYP) isoforms increase in liver in response to chemical stress, infection, or the presence of transgenes,[13–15] and CYP enzymes may release ROS,[16] we examined the livers at relatively advanced stages of the disease by immunohistochemistry for the amount and distribution of CYP1A and CYP2A5 isoforms. Both exhibited pronounced up-regulation as part of the hepatitis particularly in regions with heavy leukocytic infiltrates. Additionally, the CYP2A5 co-localized in hepatocytes where formazan deposits from NBT indicated ROS generation. Three glutathione *S*-transferase (GST) isoforms also exhibited dramatic increases.

Materials and Methods

H. hepaticus-*Infected and Control Mice*

Naturally infected A/JNCr have been maintained at FCRDC for experimental purposes. Controls were A/J mice from The Jackson Laboratory (Bar Harbor, ME) and *H. hepaticus*-free A/JNCr mice bred at FCRDC as indicated for specific experiments. For experimental infection, A/JNCr mice, aged 4 weeks, were intubated with 0.5 ml of a suspension containing approximately 10^8 bacteria (strain 2) as described previously.[17] Age-matched controls maintained in parallel in a *Helicobacter*-free room were intubated with saline.

Measurement of 8-oxo-dG

DNA was extracted from the nuclear fraction of liquid nitrogen-frozen livers and hydrolyzed to nucleosides as described by Adachi et al,[18] except that incubation times with nuclease P-1 (Sigma, St. Louis, MO) and alkaline phosphatase (Sigma) were extended to 1 hour and 2 hours, respectively. 8-Oxo-dG was quantified with an ESA500 electrochemical HPLC system with a Coulochem II multielectrode detector (ESA, Chelmsford, MA). Chromatography was performed at 1 ml/minute flow rate with 100 mmol/L sodium acetate (Sigma) in 2% methanol (Burdick and Jackson, Muskegon, MI) as an eluent.

For each experimental set, one or two lobes of each of three to five livers were analyzed separately, and all values were averaged. Similar statistical results were obtained based on averages for each animal. Tests included Student's *t*-test, and, for changes with time, linear regression analysis or the Spearman's rank correlation test for line slope data with similar and dissimilar variances, respectively.

Liver Perfusion with Nitro Blue Tetrazolium

This procedure was carried out as described by Hagen et al.[12] Briefly, blood was removed from the livers by retrograde perfusion of Hanks' balanced salt solution into the heart, and the livers were then perfused with NBT (1 mg/ml) for 20 minutes at 2 ml/minute, followed by removal of unreacted NBT by postperfusion with the salt solution. The perfused livers were fixed in zinc/formalin.

Pathology and Immunohistochemistry

Livers were fixed in 10% buffered formalin, embedded in paraffin, sectioned at 5 μm, and stained with hematoxylin and eosin for pathological diagnoses. For immunohistochemistry as described previously,[14] deparaffinized, rehydrated sections were incubated overnight (4°C) with antibodies to CYP1A (1:1000),[19] CYP2A5 (1:750),[20] mGSTP1–1 (GST pi) (1:2500, generously provided by Dr. M. Tsuda), mGSTA1–1 (GST YaYa), (1:600),[21] or mGSTA4–4 (1:500).[22] After washing, the sections were incubated with biotinylated goat antiserum to rabbit immunoglobulin and by the avidin biotin peroxidase-complex method (Vectastain kit, Vector Laboratories, Burlingame, CA) and then with 0.1% diaminobenzidine tetrahydrochloride in 0.1 mol/L Tris buffer, pH 7.2. Background staining was minimal with preimmune control sera under these conditions.

Immunoblotting

Immunoblotting for CYP1A1/1A2 was carried out using a polyclonal antibody to rat CYP1A (Human Biologicals, Dallas, TX) that recognizes both isoforms. Microsomal proteins (2 μg) were electrophoresed on 8% precast minigels (Novex Corp., Richmond VA), transferred to nitrocellulose membranes, and incubated with a 1:5000 dilution of the antibody. Microsomes from livers of Swiss mice treated with 2,3,7,8-tetrachlorodibenzo-*p*-dioxin (TCDD) were included as a positive control and as an indicator of the exact positions of CYP1A1 and CYP1A2. Bands were visualized using a goat anti-rabbit alkaline phosphatase conjugated IgG (Life Technologies Inc., Gaithersburg, MD).

Results

8-oxo-dG in Hepatic Nuclear DNA

Levels of 8-oxo-dG were greater in livers of mice naturally infected with *H. hepaticus* at 10 to 18 months of age

Table 1. Oxidative DNA Damage in Livers Naturally Infected with *H. hepaticus* and Age-Matched Control Livers

Parameter	8-oxo-dG per 10^5 dG ± SE (*N*)		
	Infected	Control	*P*
Series 1 age			
12 months	1.81 ± 0.11 (5)	1.17 ± 0.10 (6)	0.001*
18 months	2.56 ± 0.38 (6)	1.51 ± 0.17 (6)	0.025*
Series 2 age			
10 months	1.25 ± 0.31 (5)	0.91 ± 0.13 (3)	NS
18 months	2.47 ± 0.90 (4)	Not done	
Age-related effects, series 1 and 2			
Average *vs* time, line slope	0.023	0.0068	
95% confidence interval	−0.001 to 0.048	0.0015 to 0.012	
Significance *vs* 0	0.024†	0.015§	

*Significance of difference, infected *vs* control livers, Student's *t*-test.
†Spearman's rank correlation test.
§Linear regression analysis.
Infected mice were A/JNCr and control mice were A/J, maintained in parallel but in a separate room. The livers for series 2 had been perfused with NBT (see text).

compared with controls (Table 1) with differences of statistical significance at 12 and 18 months and with a significant time-dependent increase. Good agreement was found in two different experimental series. Levels of 8-oxo-dG also increased significantly with age in the control livers but at a rate that was approximately one-third that for the infected mice (Table 1). Thus, the average increase in oxidative DNA damage in the infected livers, relative to controls, became more pronounced with time: 37% at 10 months, 55% at 12 months, and 69% at 18 months (values from series 1 and series 2 combined).

To confirm that oxidative liver DNA damage can be definitively linked to *H. hepaticus* infection and to test whether it occurs early in the infection process, mice were experimentally infected with the bacterium and liver DNA extracted after 2, 4, or 12 weeks. Significant differences were seen at all time points (Table 2). Again, the rate of age-related increase was less in controls than in infected mice.

In Situ *Localization of Radical Formation by NBT Perfusion*

To determine the cell type in which superoxide was generated, livers of control and *Helicobacter*-exposed mice were perfused with NBT. In uninfected mice, blue formazan staining was observed in occasional hepatocytes with a few granules in adjacent cells (Figure 1A). In perfused livers of 10-month-old mice with hepatitis, there were focal areas with numerous hepatocytes showing intense formazan accumulation, especially in periportal areas in association with early stages of leukocytic infiltration (Figure 1B). The five livers of 18-month-old mice all exhibited characteristic hepatitis, inflammation, and preneoplastic or neoplastic lesions. Widespread areas of hepatocytes containing cytoplasmic formazan occurred in association with portal triads and leukocytic infiltrates (Figure 1, C and D). Neutrophils and macrophages were uncommon in these infiltrates, and neither they nor Kupffer cells showed formazan deposits.

Immunohistochemical Determination of Cytochrome P450

To determine whether the increase in DNA-damaging radicals in *H. hepaticus*-infected livers related to an increase in CYP isoforms, immunohistochemistry was performed for CYP1A and CYP2A5. For CYP1A, control livers presented symmetrical, uniform centrilobular staining (Figure 2A). By contrast, infected livers with inflammation showed a marked increase in degree and extent of staining, including periportal regions (Figure 2B). Particularly strong staining was sometimes observed in hepatocytes in the vicinity of leukocytic infiltrates. Normal parenchyma adjacent to adenomas was strongly positive for CYP1A,

Table 2. Oxidative DNA Damage in Livers of Mice Experimentally Infected with *H. hepaticus* and Age-Matched Control Livers

Parameter	8-oxo-dG per 10^5 dG ± SE (*N*)		
	Infected	Control	*P*
Time after infection			
2 weeks	1.31 ± 0.12 (6)	0.82 ± 0.11 (4)	0.015*
4 weeks	1.33 ± 0.13 (6)	0.86 ± 0.03 (4)	0.0075*
12 weeks	2.11 ± 0.19 (6)	1.20 ± 0.13 (5)	0.003*
Age-related effects			
Average *vs* time, line slope	0.0084	0.0040	
95% confidence interval	0.0042 to 0.012	0.001 to 0.0069	
Significance *vs* 0†	0.0006	0.011	

*Infected *vs* control, Student's *t*-test.
†Linear regression analysis.
All mice were A/JNCr.

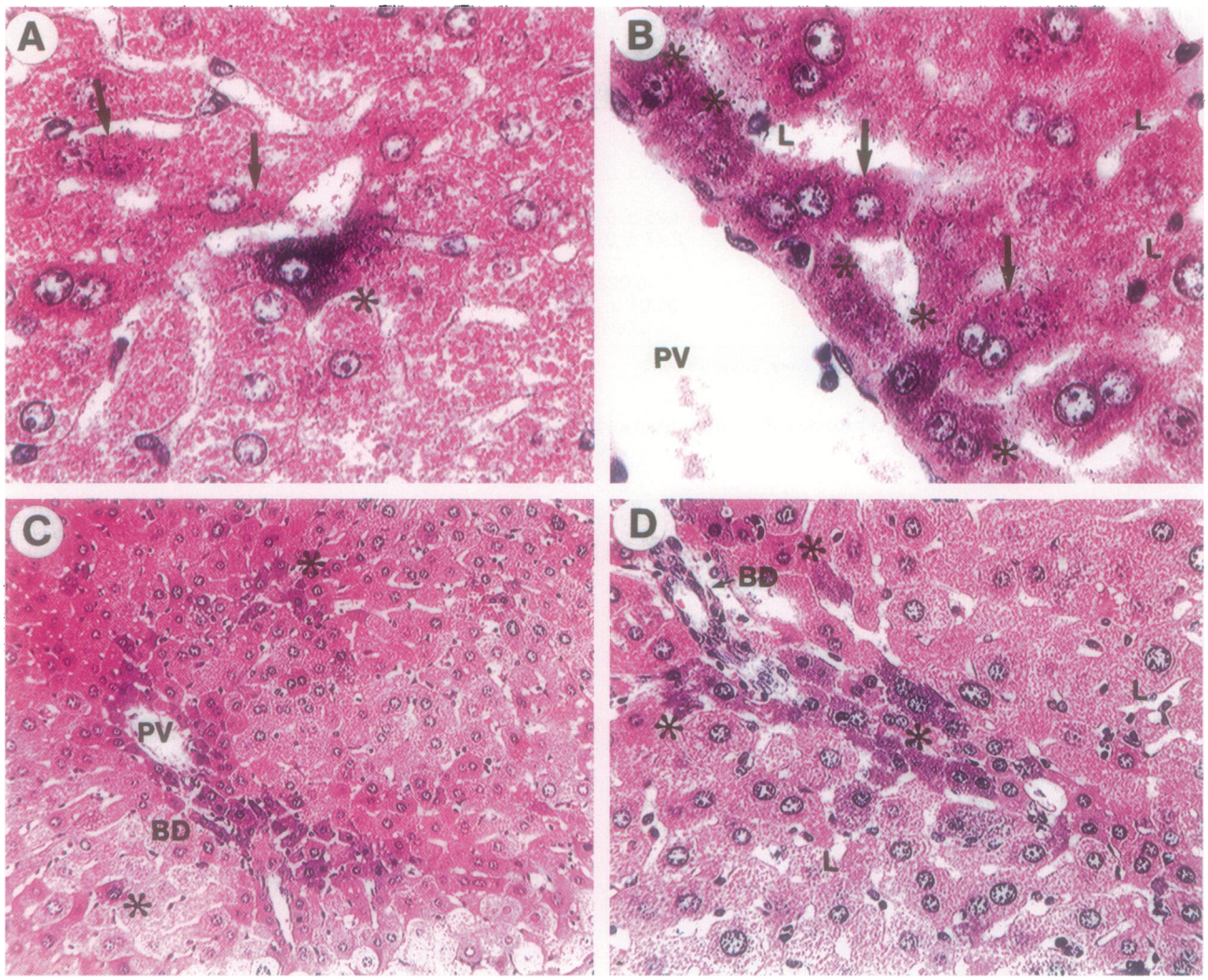

Figure 1. Production of superoxide in hepatocytes as indicated by formazan precipitates after NBT perfusion. **A:** In a control liver, age 10 months, there are dark blue staining (**asterisk**) and scattered granules (**arrows**) caused by formazan deposits in hepatocyte cytoplasm. Magnification, ×300. **B:** In an infected liver, age 10 months, there are dense formazan deposits (**asterisks**) in all cells adjacent to the portal vein (**PV**) in addition to granules in many cells in the next layer (**arrows**) and numerous leukocytes (**L**). Magnification, ×300. **C:** In an infected liver, age 18 months, there is extensive formazan deposition near the portal triad (**BD**, bile duct) and some distance away (**asterisks**). Magnification, ×75. **D:** An area of the liver, illustrated in **C**, is shown at higher power with groups of NBT-reactive cells (**asterisks**) near the bile duct and in association with many leukocytes. Magnification, ×150.

whereas most tumor cells stained minimally (Figure 2C). An 18-month-old mouse that was exposed to *H. hepaticus* but developed only mild hepatitis showed only minor changes in CYP1A expression, confirming the specific association of these alterations with the liver pathology (data not shown). Although the antibody used for these studies recognizes both CYP1A1 and CYP1A2, only CYP1A2 was detected in control and infected livers by immunoblotting analysis with an increase apparent in infected livers (Figure 3).

For CYP2A5 in control livers, highest staining occurred in the hepatocyte layer immediately adjacent to the central veins (Figure 2D). Nuclear staining was apparent in occasional cells with intensity greater than that in the cytoplasm (Figure 2D, arrows). In severely infected livers, a striking increase in the amount and extent of expression of CYP2A5 was observed, particularly in the vicinity of leukocyte accumulations (Figure 2E). Some nuclei were markedly positive for CYP2A5 (Figure 2E, arrows). A twofold increase in coumarin 7-hydroxylase activity, a specific marker for CYP2A5, and a three to fivefold elevation in CYP2A5 mRNA in Northern blots confirmed these immunohistochemical findings and have been reported in an another publication.[23] In contrast to CYP1A, CYP2A5 was present in tumor as well as in normal cells (Figure 2F).

Co-Localization of Formazan and CYP Proteins

To test for a relationship between increased CYP proteins and ROS generation leading to formazan precipitate, sections of NBT-perfused livers were immunostained with antibodies to CYP1A or CYP2A5. Sections from a liver lobe presenting a high level of 8-oxo-dG (5.2 8-oxo-dG/10^5 G) are illustrated (Figure 4). Formazan and

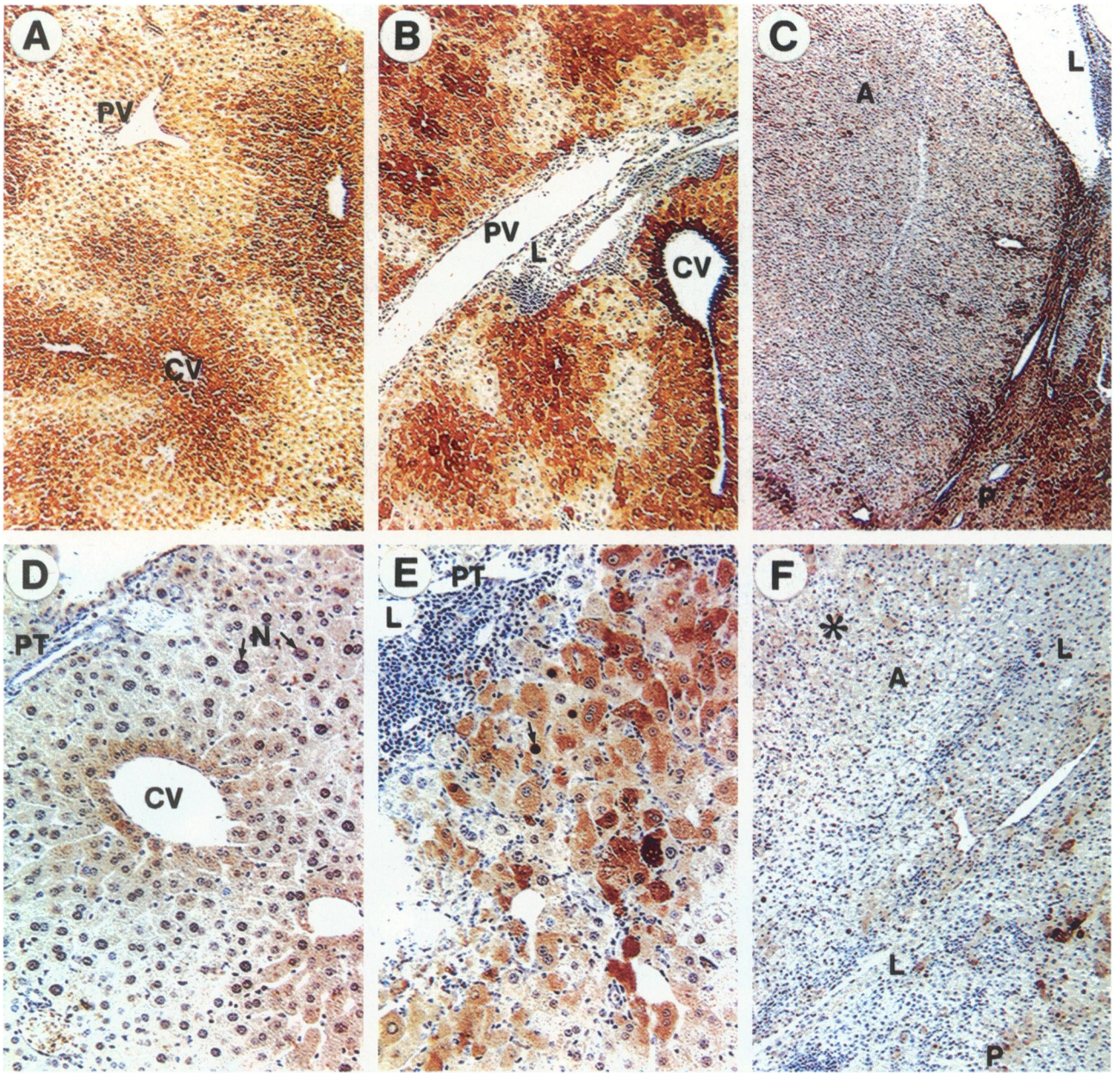

Figure 2. Immunohistochemical staining for CYP1A2 and CYP2A5, livers of mice age 18 months. **A:** In a control stained with anti-CYP1A, there is moderate symmetrical staining around the central veins (**CV**) but little around the portal vein. Magnification, ×75. **B:** In an infected liver, anti-CYP1A gives increased intensity of staining and more hepatocytes involved, including those near leukocytic infiltrates and portal triads. Magnification, ×75. **C:** An adenoma (**A**) and surrounding parenchyma (**P**) with adjacent leukocytic infiltrate are illustrated. Normal hepatocytes are intensely stained, but with most of the tumor showing less CYP1A. Magnification, ×30. **D:** In a control liver stained with anti-CYP2A5, cytoplasmic CYP2A5 is localized mainly around the central veins and is absent in region of the portal triad (**PT**); some nuclear staining is evident (**N, arrows**). Magnification, ×150. **E:** In an infected liver, anti-CYP2A5 stains more intensely and involves more cells, compared with the control (**D**), and occurs adjacent to a leukocytic infiltrate surrounding a portal triad. Some of the nuclear staining is dense (**arrow**). Magnification, ×150. **F:** Anti-CYP2A5 staining of the adenoma illustrated in **C** reveals positive areas (**asterisk**). Magnification, ×75.

increased CYP1A expression occurred in the same area but typically in different cells (Figure 4A). A small proportion of cells clearly showed both the blue formazan crystals and the brown staining caused by CYP1A (Figure 4, A and B, arrows).

By contrast, almost all of the cells in this liver lobe characterized by abnormal expression of CYP2A5 near portal triads, also were sites of formazan formation: in Figure 4, C and D, most cells contain varying mixtures of brown (CYP) and blue (formazan) stain. Thus, much of the superoxide seemed to have been generated in cells also expressing appreciable levels of CYP2A5.

Immunohistochemical Staining for GST Proteins

In 18-month control livers, staining was prominent for mGSTP1–1 periportally (Figure 5A), weak for mGSTA1–1 in the centrilobular region (Figure 5B), and moderate for mGSTA4–4 throughout the parenchyma, especially cen-

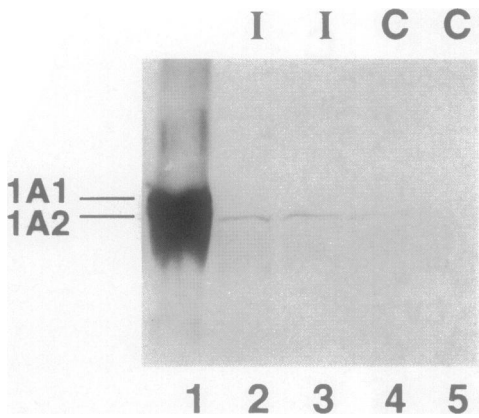

Figure 3. Western immunoblot for CYP1A2. The results show increased levels of CYP1A2, but not of CYP1A1 in infected livers. **Lane 1:** TCDD-induced mouse liver microsomes were used to show the positions of CYP1A1 and CYP1A2. **Lanes 2** and **3:** Microsomes from livers of 18-month-old *H. hepaticus*-infected mice. Those in **lane 2** are from the liver illustrated in Figure 2. **Lanes 4** and **5:** Control liver microsomes from 18-month-old mice.

trilobularly (Figure 5C). Pronounced increases in amount and distribution of all three isoforms occurred in severely infected livers near leukocytic infiltrates (Figure 5, D to F).

Discussion

The consistent, significant, time-related increase in 8-oxo-dG in livers of *H. hepaticus*-infected mice compared with age-matched controls confirms the potential role of infection-associated ROS in tumorigenesis, as frequently postulated.[3,9,10] Recently, increased levels of 8-oxo-dG were demonstrated in human livers with chronic hepatitis[24] and in *H. pylori*-infected human gastric mucosa.[25]

A striking finding in our study was that ROS apparently were not produced by the inflammatory nonparenchymal cells: the perfusion studies showed clearly that the NBT-reactive superoxide was generated in the hepatocytes. Similar outcomes occurred in carbon tetrachloride-intox-

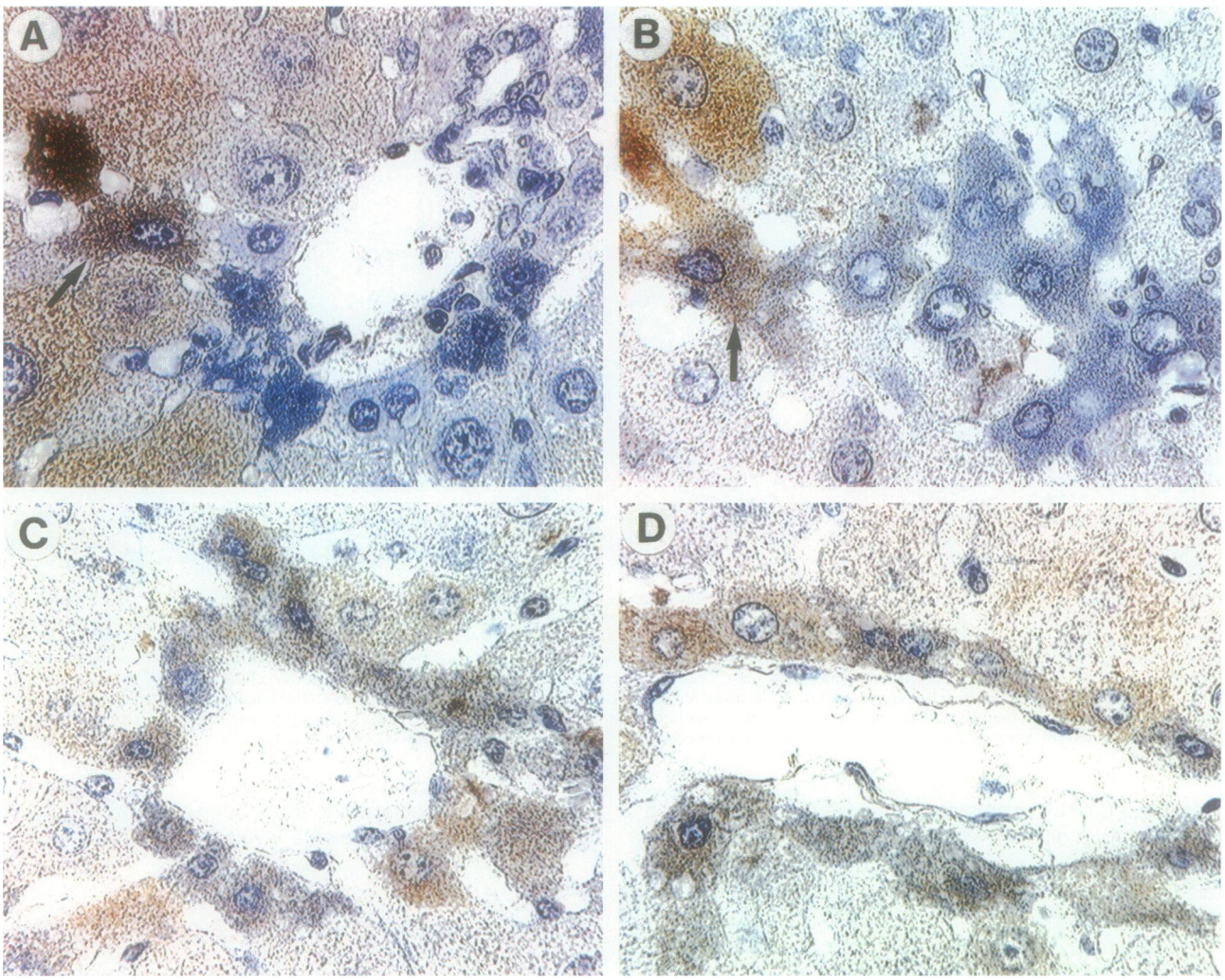

Figure 4. NBT perfusion followed by anti-CYP immunostaining to test for co-localization of formazan from superoxide and increased levels of CYP. **A** and **B:** Anti-CYP1A. Many hepatocytes presented pronounced blue formazan or brown staining, indicating CYP1A; occasional hepatocytes (**arrows**) showed combined staining. **C** and **D:** Anti-CYP2A5. Hepatocytes surrounding a section of portal vein all stained for CYP2A5; many of them were positive for formazan also. No cells were positive for formazan only in these fields; compare with **A** and **B**. Magnification, ×300).

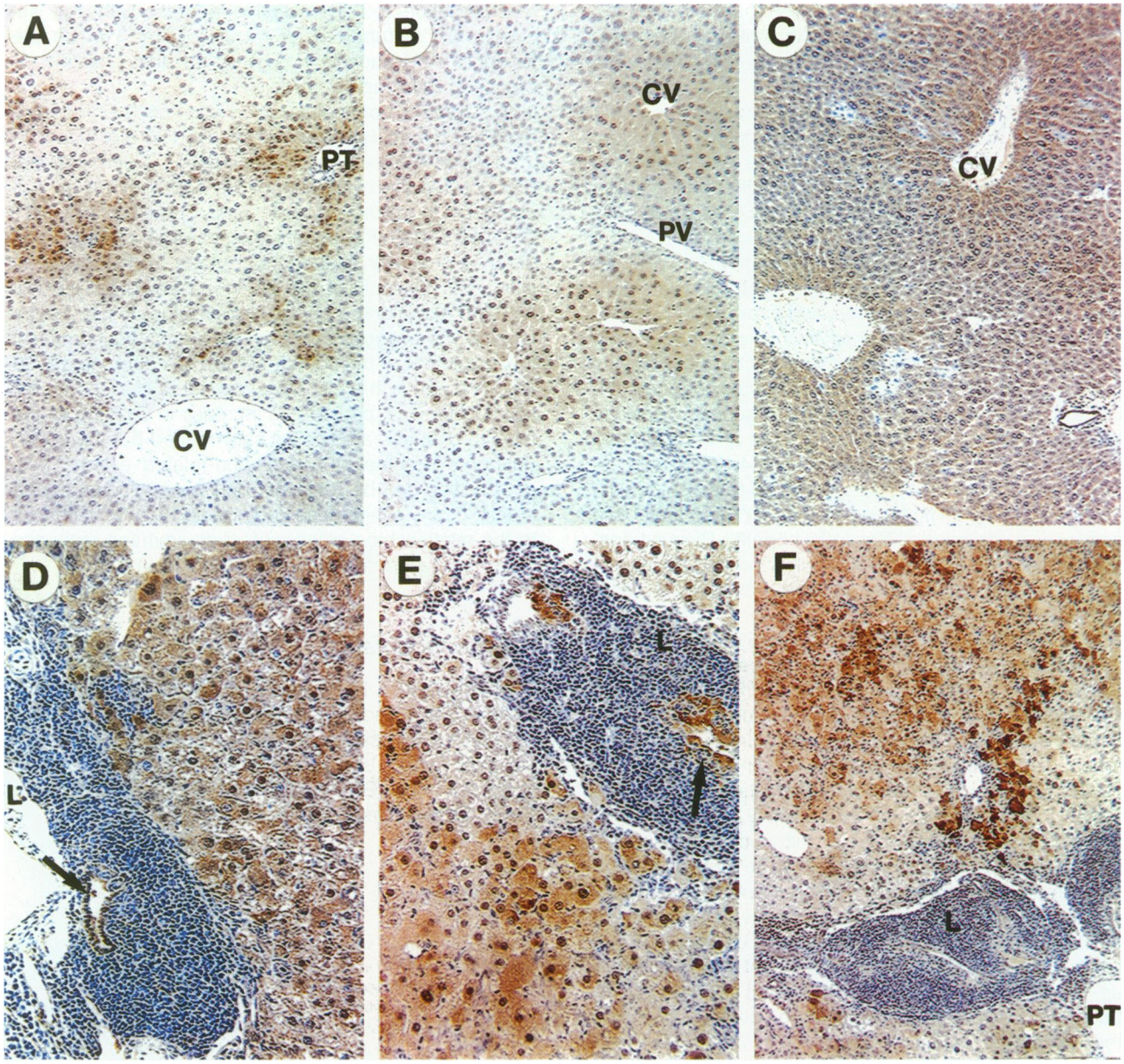

Figure 5. Immunohistochemical staining for GST isoforms in livers of mice age 18 months. **A:** In a control liver, staining caused by anti-mGSTP1–1 is localized to the portal triad regions. Magnification, ×75). **B:** In a control liver, staining caused by anti-mGSTA1–1 is largely centrilobular. Magnification, ×75. **C:** In a control liver, staining caused by anti-mGSTA4–4 is generalized but most intense in the centrilobular region. Magnification, ×75. **D:** In an infected liver, staining with anti-GST pi is intense in the cytoplasm and nuclei in all hepatocytes near a periportal leukocytic infiltrate; the bile duct epithelium also stained (**arrow**). Magnification, ×150. **E:** In an infected liver, staining with anti-GST YaYa reveals prominent cytoplasmic and nuclear staining of hepatocytes adjacent to an accumulation of leukocytes and hypertrophic bile duct epithelium (**arrow**). Magnification, ×150. **F:** In an infected liver, staining with anti-mGSTA4–4 reveals high expression near leukocytic focus surrounding portal triad and in hepatocytes with numerous interspersed leukocytes (**upper left**). Magnification, ×75.

icated rats[11] and in HBV-transgenic mice 4 to 6 months of age.[12] In contrast to gastric mucosa infected with *H. pylori*,[3] in which neutrophils and macrophages are common, the host response in *H. hepaticus*-infected livers of our series consisted almost entirely of mononuclear cells, which were uniformly negative for formazan.

One possible source of ROS was induced CYP enzymes that have the potential to release superoxide and/or cause oxidative damage of cellular molecules.[16,26] This can occur even in the absence of added substrate and has been demonstrated for CYP1A1 and CYP1A2,[26] CYP2B[26–28] and CYP2E1.[28,29] In general, hepatic CYPs decrease during parasitic and bacterial infections, exposure to inflammatory mediators, and chemical toxic injury.[30–32] However, regulation of CYP2A5 is a clear exception: this isoform typically increases during all sorts of hepatic stress,[13–15] including mice transgenic for the hepatitis B virus and experiencing hepatitis and liver tumorigenesis[13] and livers of male hamsters infected with flukes.[14] In the latter, CYP2A5 was up-regulated especially in hepatocytes adjacent to areas of inflammation. Similarly, the human homologue CYP2A6 was increased in hepatocytes adjacent to cirrhosis-caused fibrotic areas.[33]

Our immunohistochemistry showed that both CYP1A2 and CYP2A5 were up-regulated, with striking co-localization of formazan and CYP2A5. There are several possible interpretations of this correlative finding. ROS generated by an unknown source within these hepatocytes could have led to CYP2A5 induction as well as NBT reduction. Alternatively, CYP2A5, up-regulated as part of the hepatic stress response, released ROS. Although the ability of the CYP2A5 isoform to generate ROS has apparently not been investigated, our findings are consistent with it doing so. Infection-associated generation of ROS, as indicated by formazan deposits after NBT perfusion, generally occurred in hepatocytes also expressing CYP2A5 and in close proximity to leukocytic infiltrates, suggesting a link among these three phenomena. One possibility is that cytokines produced by lymphocytes induced the CYP2A5, which then released ROS. In general cytokines down-regulate CYP expression in liver and in cultured hepatocytes.[31,32] However, interleukin-4 specifically induced expression of CYP2E1,[31] and, in rats treated with interleukin-2, a significant increase in CYP2A5 metabolic activity was observed.[34] Recently, hepatitis B virus transgenic mice, injected with cytotoxic T cells, a potential source of cytokines, also showed increases in both CYP2A5 and CYP1A.[35]

Also of interest with regard to CYP2A5 are the increase in nuclear levels in infected livers and persistent expression in tumors, as reported previously,[36] confirming the likelihood of ROS, if generated by this enzyme, causing tumor initiation and progression, respectively. The occurrence of nuclear CYPs, a classical finding,[37] has received relatively little attention despite its obvious importance in the context of genotoxicity. Specific CYP isoforms recently described in the nucleus of various cells include 1A1, 1A2, and 2B;[38,39] generation of ROS by isolated nuclei has been demonstrated.[40] Not all cells positive for CYP2A5 were also formazan stained. Clearly other factors are operative, and it may be that GST isoforms (see below) or other antioxidant enzymes were up-regulated in some cells to counteract increased ROS. Such concomitant protective changes could also explain the lack of NBT-detected superoxide in many cells showing increased CYP1A2, despite the known ability of this isoform to leak superoxide.[26]

The marked increase in one P and several A class GST isoforms in livers with advanced *Helicobacter* hepatitis and concomitant elevation in ROS is consistent with the known induction of these enzymes by stress and ROS and their affinity for substrates that are products of ROS action.[41] The A form mGSTA4–4 is associated especially with oxidative damage,[42] having a high affinity for lipid peroxidation products.[22] GSTA1 and GSTA2 isoforms were up-regulated by interleukin-4 in primary human hepatocyte cultures.[43] The P isoform is proposed to act as a redox sensor.[44] Thus, cytokines may induce both GST and CYP isoforms in some hepatocytes. A concomitant induction of superoxide dismutase could explain the absence of pronounced formazan staining in many CYP-positive cells (see above).

8-oxo-dG increased with age in both control and *H. hepaticus*-infected livers at a significantly faster rate in the latter as expected. The relative increase with age was similar to that reported for rat liver DNA,[45] which was thought to be caused in part by an aging-related decrease in DNA repair capacity.

In summary, both natural and experimental infection of male mice with *H. hepaticus* resulted in significant increases in 8-oxo-dG in nuclear DNA. Superoxide was produced in the cytoplasm of the hepatocytes, as indicated by formazan deposits after perfusion with NBT. CYP1A2 and CYP2A5 were increased in infected livers often in proximity to the portal triads and plasmacytic infiltrates. Co-localization of formazan deposits with CYP2A5 and marked nuclear localization of this enzyme in some cells suggested that infection-related increase in this enzyme was the source of the DNA-damaging ROS. As noted above, it is also possible that ROS, generated in some other way, caused the increase in CYP2A5 or that the two changes are not causally related but the consequences of some other infection-related event. These possibilities can be ruled out only by additional experiments. In any event these findings add a new dimension to the relationships among infection, immune response, reactive oxygen, and cancer causation.

Acknowledgments

We thank Drs. M. Lang and M. A. Hayes for the antibodies to CYP2A5 and GST YaYa, respectively; M. Laval and N. Lynadrat for assistance with the immunohistochemical staining; Daniel Logsdon for liver perfusions; Barbara Kasprzak for mGSTA4–4 immunohistochemistry; and Laura Fornwald for immunoblotting.

References

1. Hepatitis viruses. International Agency for Research on Cancer Monographs on the Evaluation of Carcinogenic Risk to Humans, vol 59. IARC, 1994, pp 1–255
2. Schistosomes, liver flukes, and *Helicobacter pylori*. International Agency for Research on Cancer Monographs on the Evaluation of Carcinogenic Risk to Humans, vol 61. IARC, 1994, pp 1–239
3. Correa P: *Helicobacter pylori*, and gastric carcinogenesis. Am J Surg Pathol 1995, 19 (Suppl. 1):S37–S43
4. Ward JM, Fox JG, Anver MR, Haines DC, George CV, Collins MJ, Gorelick PL, Nagashima K, Gonda MA, Gilden RV, Tully JG, Russell RJ, Benveniste RE, Paster BJ, Dewhirst FE, Donovan JC, Anderson LM, Rice JM: Chronic active hepatitis and associated liver tumors in mice caused by a persistent bacterial infection with a novel *Helicobacter* species. J Natl Cancer Inst 1994, 86:1222–1227
5. Fox JG, Dewhirst FE, Tully JG, Paster BJ, Yan L, Taylor NS, Collins MJ, Gorelick PL, Ward JM: *Helicobacter hepaticus sp nov*, a microaerophilic bacterium isolated from livers, and intestinal mucosal scrapings from mice: J Clin Microbiol 1994, 32:1238–1245
6. Ward JM, Anver MR, Haines DC, Benveniste RE: Chronic active hepatitis in mice caused by *Helicobacter hepaticus*. Am J Pathol 1994, 146:959–968
7. Rice JM: *Helicobacter hepaticus*, a recently recognized bacterial pathogen, associated with chronic hepatitis, and hepatocellular neoplasia in laboratory mice: Emerg Infect Dis 1995, 1:129–131
8. Fox JG, Li X, Yan L, Cahill RJ, Hurley R, Lewis R, Murphy JC: Chronic proliferative hepatitis in A/JCr mice associated with persistent *Helicobacter hepaticus* infection: a model of Helicobacter-induced carcinogenesis. Infect Immun 1996, 64:1548–1558
9. Clayson DB, Mehta R, Iverson F: Oxidative DNA damage - the effects

of certain genotoxic, and operationally non-genotoxic carcinogens: Mutat Res 1994, 317:25–42
10. Marnett LJ: Peroxy free radicals: potential mediators of tumor initiation and promotion. Carcinogenesis 1987, 8:1365–1373
11. Mochida S, Masaki N, Ohta Y, Matsui A, Ogata I, Fujiwara F: *In situ* detection of oxidative stress in rat hepatocytes. J Pathol 1992, 167: 83–89
12. Hagen TM, Huang S, Curnutte J, Fowler P, Martinez V, Wehr CM, Ames BN, Chisari FV: Extensive oxidative DNA damage in hepatocytes of transgenic mice with chronic active hepatitis destined to develop hepatocellular carcinoma. Proc Natl Acad Sci USA 1994, 91:12808–12812
13. Kirby GM, Chemin I, Montesano R, Chisari FV, Lang MA, Wild CP: Induction of specific cytochrome P450s involved in aflatoxin B_1 metabolism in hepatitis B virus transgenic mice. Mol Carcinogen 1994, 11:74–80
14. Kirby GM, Pelkonen P, Vatanasapt V, Camus A, Wild CP, Lang MA: Association of liver fluke (*Opisthorchis viverrini*) infestation with increased expression of cytochrome P450 and carcinogen metabolism in male hamster liver. Mol Carcinogen 1994, 11:81–89
15. Camus-Randon A, Raffalli F, Bereziat J, McGregor D, Konstandi M, Lang MA: Liver injury and expression of cytochromes P450: evidence that regulation of CYP2A5 is different from that of other major xenobiotic metabolizing CYP enzymes. Toxicol Appl Pharmacol 1996, 138:140–148
16. Bondy SC, Naderi S: Contribution of hepatic cytochrome P450 systems to the generation of reactive oxygen species. Biochem Pharmacol 1994, 48:155–159
17. Canella KA, Diwan BA, Gorelick PL, Donovan PJ, Sipowicz MA, Kasprzak KS, Weghorst CM, Snyderwine EG, Davis CD, Keefer LK, Kyrtopoulos SA, Hecht SS, Wang M, Anderson LM, Rice JM: Liver tumorigenesis by *Helicobacter hepaticus*: considerations of mechanism. In Vivo 1996, 10:285–292
18. Adachi S, Zeisig M, Moller L: Improvements in the analytical method for 8-hydroxydeoxyguanosine in nuclear DNA. Carcinogenesis 1995, 16:253–258
19. Honkakoski P, Lang, M: Mouse liver phenobarbital-inducible P450 system: purification, characterization and differential inducibility of four cytochrome P450 isoenzymes from the D2 mouse. Arch Biochem Biophys 1989, 273:42–57
20. Lang MA, Juvonen R, Jarvinen P, Honkakoski P, Raunio H: Mouse liver P450Coh: genetic regulation of the pyrazole-inducible enzyme and comparison with other P450 isoenzymes. Arch Biochem Biophys 1989, 271:139–148
21. Quinn BA, Crane TL, Kocal TE, Best SJ, Cameron RG, Rushmore TH, Farber E, Hayes MA: Protective activity of different hepatic cytosolic glutathione S-transferases against DNA-binding metabolites of aflatoxin B_1. Toxicol Appl Pharmacol 1990, 105:351–363
22. Zimniak P, Singhal SS, Srivastava SK, Awasthi S, Sharma R, Hayden JB, Awasthi YC: Estimation of genomic complexity, heterologous expression, and enzymatic characterization of mouse glutathione S-transferase mGSTA4–4 (GST5.7). J Biol Chem 1994, 269:992–1000
23. Chomarat P, Sipowicz MA, Diwan BA, Fornwald LW, Kasprzak KS, Awasthi YC, Anver MA, Ward JM, Rice JM, Anderson LM, Wild CP: Distinct time courses of increase in cytochromes P450 1A2, 2A5, and glutathione S-transferases during the progressive hepatitis associated with *Helicobacter hepaticus*. Carcinogenesis (in press)
24. Shimoda R, Nagashima M, Sakamoto M, Yamaguchi N, Hirohashi S, Yokota J, Kasai H: Increased formation of oxidative DNA damage, 8-hydroxydeoxyguanosine, in human livers with chronic hepatitis. Cancer Res 1994, 54:3171–3172
25. Baik S, Youn H, Chung M, Lee W, Cho M, Ko G, Park C, Kasai H, Rhee K: Increased oxidative DNA damage in *Helicobacter pylori*-infected human gastric mucosa. Cancer Res 1996, 56:1279–1282
26. Morehouse LA, Aust SD: Generation of superoxide by the microsomal mixed-function oxidase system. Basic Life Sci 1988, 49:517–521
27. Puntarulo S, Cederbaum AI: Role of cytochrome P-450 in the stimulation of microsomal production of reactive oxygen species by ferritin. Biochim Biophys Acta 1996, 289:238–246
28. Ekstrom G, Ingelman-Sundberg M: Rat liver microsomal NADPH-supported oxidase activity and lipid peroxidation dependent on ethanol-inducible cytochrome P-450 (P-450IIE1). Biochem Pharmacol 1989, 38:1313–1319
29. Dai Y, Rashba-Step J, Cederbaum AI: Stable expression of human cytochrome P4502E1 in HepG2 cells: characterization of catalytic activities and production of reaction oxygen intermediates. Biochemistry 1993, 32:6928–6937
30. Proulx M, du Souich P: Inflammation-induced decrease in hepatic cytochrome P450 in conscious rabbits is accompanied by an increase in hepatic oxidative stress. Res Commun Mol Pathol Pharmacol 1995, 87:221–236
31. Abdel-Razzak Z, Loyer P, Fautrel A, Gautier J, Corcos L, Turlin B, Beaune P, Guillouzo A: Cytokines down-regulate expression of major cytochrome P-450 enzymes in adult human hepatocytes in primary culture. Mol Pharmacol 1993, 44:707–715
32. Tinel M, Robin M, Doostzadeh J, Maratrat M, Ballet F, Fardel N, El Kahwaji J, Beaune P, Daujat M, Labbe G, Pessayre D: The interleukin-2 receptor down-regulates the expression of cytochrome P450 in cultured rat hepatocytes. Gastroenterology 1995, 109:1589–1599
33. Palmer CNA, Coates PJ, Davies SE, Shephard EA, Phillips IR: Localization of expression of cytochrome P-450 gene expression in normal and diseased human liver by in situ hybridization of wax-embedded archival material. Hepatology 1992, 16:682–687
34. Kurokohchi K, Matsuo Y, Yoneyama H, Nishioka M, Ichikawa Y: Interleukin 2 induction of cytochrome P450-linked monooxygenase systems of rat liver microsomes. Biochem Pharmacol 1993, 45:585–592
35. Chemin I, Takahashi S, Belloc C, Lang MA, Ando K, Guidott LG, Chisari FV, Wild CP: Differential induction of carcinogen metabolizing enzymes in a transgenic mouse model of fulminant hepatitis. Hepatology 1996, 24:649–656
36. Kobliakov V, Kulikova L, Samoilov D, Lang MA: High expression of cytochrome P450 2a-5 (coumarin 7-hydroxylase) in mouse hepatomas. Mol Carcinogen 1993, 7:276–280
37. Bresnick E: Nuclear activation of polycyclic hydrocarbons. Drug Metab Rev 1979, 10:209–223
38. Carubelli R, Graham SA, McCay PB, Friedman FK: Prevention of 2-acetylaminofluorene-induced loss of nuclear envelope cytochrome P450 by the simultaneous administration of 3-methylcholanthrene. Biochem Pharmacol 1991, 41:1331–1334
39. Madra S, Mann F, Francis JE, Manson MM, Smith AG: Modulation by iron of hepatic microsomal and nuclear cytochrome P450, and cytosolic glutathione S-transferase and peroxidase in C57BL/10ScSn mice induced with polychlorinated biphenyls (Aroclor 1254). Toxicol Appl Pharmacol 1996, 136:79–86
40. Puntarulo S, Cederbaum AI: Effect of phenobarbital and 3-methylcholanthrene treatment on NADPH- and NADH-dependent production of reactive oxygen intermediates by rat liver nuclei. Biochim Biophys Acta 1992, 1116:17–23
41. Hayes JD, Pulford DJ: The glutathione S-transferase supergene family: regulation of GST and the contribution of the isoenzymes to cancer chemoprotection and drug resistance. Crit Rev Biochem Mol Biol 1995, 30:445–600
42. Khan MF, Srivastava SK, Singhal SS, Chaubey M, Awasthi S, Petersen DR, Ansari GAS, Awasthi YC: Iron-induced lipid peroxidation in rat liver is accompanied by preferential induction of glutathione S-transferase 8–8 isozyme. Toxicol Appl Pharmacol 1995, 131:63–72
43. Langouet S, Corcos L, Abdel-Razzak Z, Loyer P, Ketterer B, Guillouzo A: Up-regulation of glutathione S-transferases α by interleukin 4 in human hepatocytes in primary culture. Biochem Biophys Res Commun 1995, 216:793–800
44. Mantle TJ: The glutathione S-transferase multigene family: a paradigm for xenobiotic interactions. Biochem Soc Trans 1995, 23:423–425
45. Fraga CG, Shigenaga MK, Park J, Degan P, Ames BN: Oxidative damage to DNA during aging: 8-hydroxy-2′-deoxyguanosine in rat organ DNA and urine. Proc Natl Acad Sci USA 1990, 87:4533–4537